SUPPLEMENTARY MATERIAL FOR "Modelling the electroluminescence of atomic wires from quantum dynamics simulations"

Carlos M. Bustamante, Tchavdar N. Todorov, Esteban D Gadea, Facundo Tarasi, Lorenzo Stella, Andrew Horsfield, Damián A. Scherlis*

E-mail: damian@qi.fcen.uba.ar

Equation of motion for the density matrix coupled to a Redfield photon bath

The Hamiltonian for a multi-electronic system interacting with a photon bath can be expressed as:

$$\hat{H} = \hat{H}_e + \sum_{\mathbf{k}} \hbar\omega_{\mathbf{k}} \left(\hat{N}_{\mathbf{k}} + \frac{1}{2} \right) - \sum_{\mathbf{k}} \hat{\mathbf{E}}_{\mathbf{k}} \cdot \hat{\boldsymbol{\mu}}, \tag{1}$$

where $\hat{H}_e$ is the multi-electronic Hamiltonian, $\hat{N}_{\mathbf{k}}$ is the occupation operator of the photon with wave vector $\mathbf{k} = (k_x, k_y, k_z)$ and with its corresponding frequency $\omega_{\mathbf{k}} = ck$. $\hat{\boldsymbol{\mu}}$ is the electronic dipole moment operator and $\hat{\mathbf{E}}_{\mathbf{k}}$ is the photon electric field operator, which can be expanded as a function of the photon creator and annihilator operators ($\hat{a}^\dagger$, $\hat{a}$),

$$\hat{\mathbf{E}}_{\mathbf{k}} = -\mathrm{i} \sum_{\lambda}^{2} \boldsymbol{\epsilon}_{\mathbf{k},\lambda} \left(\frac{\hbar\omega_{\mathbf{k}}}{2\varepsilon_0 V} \right)^{1/2} (\hat{a}^\dagger_{\mathbf{k}} - \hat{a}_{\mathbf{k}}) \tag{2}$$

where we have considered the dipole approximation, $e^{\mathrm{i}\mathbf{k}\cdot\mathbf{r}} \approx 1$. The unit vectors $\boldsymbol{\epsilon}_{\mathbf{k},\lambda} = (\epsilon^x_{\mathbf{k},\lambda}, \epsilon^y_{\mathbf{k},\lambda}, \epsilon^z_{\mathbf{k},\lambda})$ were chosen to satisfy the following conditions:

$$\begin{aligned} \boldsymbol{\epsilon}_{\mathbf{k},1} &= \frac{\mathbf{e_1} \times \mathbf{k}}{|\mathbf{e_1} \times \mathbf{k}|} \\ \boldsymbol{\epsilon}_{\mathbf{k},2} &= \boldsymbol{\epsilon}_{\mathbf{k},1} \times \frac{\mathbf{k}}{|\mathbf{k}|} \end{aligned} \tag{3}$$

where $\mathbf{e_1}$ is the unit vector in the x direction. These conditions help us simplify the expression of the interaction term if we consider that $\hat{\boldsymbol{\mu}} = \hat{\mu}_x \mathbf{e_1}$,

$$\begin{aligned} \hat{\mathbf{E}}_{\mathbf{k}} \cdot \hat{\boldsymbol{\mu}} = \hat{E}^x_{\mathbf{k}} \hat{\mu}_x &= -\mathrm{i}\, \epsilon^x_{\mathbf{k},2} \left(\frac{\hbar \omega_{\mathbf{k}}}{2\varepsilon_0 V} \right)^{1/2} (\hat{a}^\dagger_{\mathbf{k}} - \hat{a}_{\mathbf{k}}) \hat{\mu}_x \\ &= -\mathrm{i} \frac{(k_z^2 + k_y^2)^{1/2}}{|\mathbf{k}|} \left(\frac{\hbar \omega_{\mathbf{k}}}{2\varepsilon_0 V} \right)^{1/2} (\hat{a}^\dagger_{\mathbf{k}} - \hat{a}_{\mathbf{k}}) \hat{\mu}_x. \end{aligned} \tag{4}$$

First, we will obtain the expression for the evolution of the multi-electronic density operator. To this purpose, we use the Liouville equation and trace over the photons ($\mathrm{Tr}_{\mathrm{ph}}\{...\}$),

$$\mathrm{i}\hbar \frac{d\hat{\rho}_e(t)}{dt} = [\hat{H}_e, \hat{\rho}_e(t)] - \sum_{\mathbf{k}} [\hat{\mu}_x, \hat{\Phi}_{\mathbf{k}}(t)] \tag{5}$$

where $\hat{\Phi}_{\mathbf{k}}(t) = \mathrm{Tr}_{\mathrm{ph}}\{\hat{E}^x_{\mathbf{k}} \rho(t)\}$. Henceforth, we replace $\hat{E}^x_{\mathbf{k}}$ and $\hat{\mu}_x$ by $\hat{E}_{\mathbf{k}}$ and $-e\hat{x}$ respectively. In order to get an expression for $\hat{\Phi}_{\mathbf{k}}(t)$ we write the exact solution for the density:

$$\hat{\rho}(t) = e^{-\frac{\mathrm{i}}{\hbar}\hat{H}_0 t} \hat{\rho}(0) e^{\frac{\mathrm{i}}{\hbar}\hat{H}_0 t} + \frac{1}{\mathrm{i}\hbar} \sum_{\mathbf{k}} \int_0^t e^{\frac{\mathrm{i}}{\hbar}\hat{H}_0(\tau - t)} [e\hat{E}_{\mathbf{k}}\hat{x}, \hat{\rho}(\tau)] e^{-\frac{\mathrm{i}}{\hbar}\hat{H}_0(\tau - t)} d\tau, \tag{6}$$

where $\hat{H}_0$ is the unperturbed Hamiltonian. Now we can write:

$$\hat{\Phi}_{\mathbf{k}}(t) = \frac{e}{\mathrm{i}\hbar} \mathrm{Tr}_{\mathrm{ph}} \left\{ \sum_{\mathbf{k}'} \int_0^t \hat{x}^{\tau - t} \hat{E}_{\mathbf{k}} \hat{E}^{\tau - t}_{\mathbf{k}'} \hat{\rho}^{\tau - t}(\tau) d\tau - \int_0^t \hat{\rho}^{\tau - t}(\tau) \hat{E}^{\tau - t}_{\mathbf{k}'} \hat{E}_{\mathbf{k}} \hat{x}^{\tau - t} d\tau \right\}, \tag{7}$$

where we used the notation $\hat{Q}^t = e^{\frac{\mathrm{i}}{\hbar}\hat{H}_0 t}\hat{Q}e^{-\frac{\mathrm{i}}{\hbar}\hat{H}_0 t}$.

Applying the decomposition $\hat{A}\hat{B} = (1/2)[\hat{A},\hat{B}] + (1/2)\{\hat{A},\hat{B}\}$, we get:

$$\begin{aligned}\hat{\Phi}_{\mathbf{k}}(t) =& \frac{e}{2\mathrm{i}\hbar}\mathrm{Tr}_{\mathrm{ph}}\sum_{\mathbf{k}'}\int_0^t [\hat{x}^{\tau-t},\hat{\rho}^{\tau-t}(\tau)]\{\hat{E}_{\mathbf{k}},\hat{E}^{\tau-t}_{\mathbf{k}'}\}d\tau \\ &+\frac{e}{2\mathrm{i}\hbar}\mathrm{Tr}_{\mathrm{ph}}\sum_{\mathbf{k}'}\int_0^t \{\hat{x}^{\tau-t},\hat{\rho}^{\tau-t}(\tau)\}[\hat{E}_{\mathbf{k}},\hat{E}^{\tau-t}_{\mathbf{k}'}]d\tau.\end{aligned} \tag{8}$$

Since

$$\hat{E}^{\tau-t}_{\mathbf{k}} = -\mathrm{i}\frac{(k_z^2+k_y^2)^{1/2}}{|\mathbf{k}|}\left(\frac{\hbar\omega_{\mathbf{k}}}{2\varepsilon_0 V}\right)^{1/2}(\hat{a}^\dagger_{\mathbf{k}}e^{\mathrm{i}\omega_{\mathbf{k}}(\tau-t)} - \hat{a}_{\mathbf{k}}e^{-\mathrm{i}\omega_{\mathbf{k}}(\tau-t)}), \tag{9}$$

we can use

$$\sum_{\mathbf{k}'}[\hat{E}_{\mathbf{k}},\hat{E}^{\tau-t}_{\mathbf{k}'}] = \mathrm{i}\frac{k_z^2+k_y^2}{|\mathbf{k}|^2}\frac{\hbar\omega_{\mathbf{k}}}{\varepsilon_0 V}\sin(\omega_{\mathbf{k}}(\tau-t)), \tag{10}$$

plus the assumption that the coupling is weak enough to consider the harmonic behaviour of the photons,

$$\mathrm{Tr}_{\mathrm{ph}}\sum_{\mathbf{k}'}\left(\{\hat{E}_{\mathbf{k}},\hat{E}^{\tau-t}_{\mathbf{k}'}\}\hat{\rho}^{\tau-t}_{\mathrm{ph}}(\tau)\right) \approx \frac{k_z^2+k_y^2}{|\mathbf{k}|^2}\frac{\hbar\omega_{\mathbf{k}}}{\varepsilon_0 V}(2N_{\mathbf{k}}(\tau)+1)\cos(\omega_{\mathbf{k}}(\tau-t)), \tag{11}$$

to finally get

$$\begin{aligned}\hat{\Phi}_{\mathbf{k}}(t) =& \frac{e\omega_{\mathbf{k}}}{2\mathrm{i}\varepsilon_0 V}\frac{k_z^2+k_y^2}{|\mathbf{k}|^2}\int_0^t [\hat{x}^{\tau-t},\hat{\rho}^{\tau-t}_e(\tau)](2N_{\mathbf{k}}(\tau)+1)\cos(\omega_{\mathbf{k}}(\tau-t))d\tau \\ &+\frac{e\omega_{\mathbf{k}}}{2\varepsilon_0 V}\frac{k_z^2+k_y^2}{|\mathbf{k}|^2}\int_0^t \{\hat{x}^{\tau-t},\hat{\rho}^{\tau-t}_e(\tau)\}\sin(\omega_{\mathbf{k}}(\tau-t))d\tau.\end{aligned} \tag{12}$$

Now we will assume that the distribution of photon modes is dense enough to replace the summation in Equation 12 by an integral and introduce the matrix χ^A and χ^B, which matrix elements are defined as

$$\chi^A_{ij} = \int_0^\infty \frac{e\omega^3_{\mathbf{k}}}{6\mathrm{i}\pi^2\varepsilon_0 c^3}(2N_{\mathbf{k}}+1)\int_0^t x^{\tau-t}_{ij}\cos(\omega_{\mathbf{k}}(\tau-t))d\tau\, d\omega_{\mathbf{k}}, \tag{13}$$

$$\chi^B_{ij} = \int_0^\infty \frac{e\omega^3_{\mathbf{k}}}{6\pi^2\varepsilon_0 c^3}\int_0^t x^{\tau-t}_{ij}\sin(\omega_{\mathbf{k}}(\tau-t))d\tau\, d\omega_{\mathbf{k}}. \tag{14}$$

Let's consider the first integral:

$$\chi_{ij}^{A} = \int_0^\infty \frac{e\omega_{\mathbf{k}}^3}{6\mathrm{i}\pi^2\varepsilon_0 c^3}(2N_{\mathbf{k}}+1)\int_0^t x_{ij}e^{\mathrm{i}\omega_{ij}(\tau-t)}\frac{e^{\mathrm{i}\omega_{\mathbf{k}}(\tau-t)}+e^{-\mathrm{i}\omega_{\mathbf{k}}(\tau-t)}}{2}d\tau\, d\omega_{\mathbf{k}}, \tag{15}$$

where the integration as a function of τ can be solved replacing $s = \tau - t$ with the following limits:

$$\begin{aligned}
&\lim_{\epsilon\to 0^+}\lim_{s\to-\infty}\frac{x_{ij}}{2}\int_s^0 e^{\mathrm{i}(\omega_{ij}+\omega_{\mathbf{k}}-\mathrm{i}\epsilon)s}+e^{\mathrm{i}(\omega_{ij}-\omega_{\mathbf{k}}-\mathrm{i}\epsilon)s}ds\\
&=\lim_{\epsilon\to 0^+}\frac{x_{ij}}{2\mathrm{i}}\left(\frac{1}{\omega_{ij}+\omega_{\mathbf{k}}-\mathrm{i}\epsilon}+\frac{1}{\omega_{ij}-\omega_{\mathbf{k}}-\mathrm{i}\epsilon}\right)\\
&=\lim_{\epsilon\to 0^+}\frac{x_{ij}}{2\mathrm{i}}\left(\frac{\omega_{ij}+\omega_{\mathbf{k}}+\mathrm{i}\epsilon}{(\omega_{ij}+\omega_{\mathbf{k}})^2+\epsilon^2}+\frac{\omega_{ij}-\omega_{\mathbf{k}}+\mathrm{i}\epsilon}{(\omega_{ij}-\omega_{\mathbf{k}})^2+\epsilon^2}\right)\\
&=\frac{x_{ij}}{2\mathrm{i}}\left(\frac{1}{\omega_{ij}+\omega_{\mathbf{k}}}+\frac{1}{\omega_{ij}-\omega_{\mathbf{k}}}+\pi\mathrm{i}\delta(\omega_{ij}+\omega_{\mathbf{k}})+\pi\mathrm{i}\delta(\omega_{ij}-\omega_{\mathbf{k}})\right).
\end{aligned} \tag{16}$$

In this way we can write

$$\chi_{ij}^{A} = -\int_0^\infty \frac{e\,x_{ij}\omega_{\mathbf{k}}^3}{12\pi^2\varepsilon_0 c^3}(2N_{\mathbf{k}}+1)\left(\frac{1}{\omega_{ij}+\omega_{\mathbf{k}}}+\frac{1}{\omega_{ij}-\omega_{\mathbf{k}}}+\pi\mathrm{i}\delta(\omega_{ij}+\omega_{\mathbf{k}})+\pi\mathrm{i}\delta(\omega_{ij}-\omega_{\mathbf{k}})\right)d\omega_{\mathbf{k}}. \tag{17}$$

Following the same steps, we can get for the second matrix the expression:

$$\chi_{ij}^{B} = -\int_0^\infty \frac{e\,x_{ij}\omega_{\mathbf{k}}^3}{12\pi^2\varepsilon_0 c^3}\left(\frac{1}{\omega_{ij}+\omega_{\mathbf{k}}}-\frac{1}{\omega_{ij}-\omega_{\mathbf{k}}}+\pi\mathrm{i}\delta(\omega_{ij}+\omega_{\mathbf{k}})-\pi\mathrm{i}\delta(\omega_{ij}-\omega_{\mathbf{k}})\right)d\omega_{\mathbf{k}}. \tag{18}$$

From here, we conserve just the Dirac deltas and discard the Lamb shift terms,

$$\begin{aligned}
\chi_{ij}^{A} &\approx -\int_0^\infty \frac{e\,x_{ij}\omega_{\mathbf{k}}^3}{12\pi^2\varepsilon_0 c^3}(2N_{\mathbf{k}}+1)\left(\pi\mathrm{i}\delta(\omega_{ij}+\omega_{\mathbf{k}})+\pi\mathrm{i}\delta(\omega_{ij}-\omega_{\mathbf{k}})\right)d\omega_{\mathbf{k}}\\
&=-\frac{\mathrm{i}\,e x_{ij}|\omega_{ij}|^3}{12\pi\varepsilon_0 c^3}(2N(|\omega_{ij}|)+1),
\end{aligned} \tag{19}$$

$$\begin{aligned}
\chi_{ij}^{B} &\approx -\int_0^\infty \frac{e\,x_{ij}\omega_{\mathbf{k}}^3}{12\pi^2\varepsilon_0 c^3}\left(\pi\mathrm{i}\delta(\omega_{ij}+\omega_{\mathbf{k}})-\pi\mathrm{i}\delta(\omega_{ij}-\omega_{\mathbf{k}})\right)d\omega_{\mathbf{k}}\\
&=\frac{\mathrm{i}\,e x_{ij}\omega_{ij}^3}{12\pi\varepsilon_0 c^3}.
\end{aligned} \tag{20}$$

In this way, we can rewrite Equation 5 as:

$$\mathrm{i}\,\hbar\frac{d\hat{\rho}_e}{dt} = [\hat{H}_e, \hat{\rho}_e] + e[\hat{x}, ([\hat{\chi}^A, \hat{\rho}_e] + \{\hat{\chi}^B, \hat{\rho}_e\})]. \tag{21}$$

In order to get the equation of motion for the one-electron density operator we need to trace over $N_e\mathrm{Tr}_{e,2,..,N_e}$, where N_e is the total number of electrons. Since we consider $\hat{H}_e$, $\hat{\chi}^A$ and $\hat{\chi}^B$ as single electron operators, tracing over the related commutators would lead to the same expression. For the case of the anti-commutator,

$$\mathrm{Tr}_{e,2,..,N_e}(\{\hat{\chi}^B, \hat{\rho}_e\}) = \{\hat{\chi}^{B(1)}(1), \hat{\rho}_e^{(1)}(1)\} + 2\mathrm{Tr}_{e,2}(\hat{\chi}^{B(2)}(2)\hat{\rho}_e^{(2)}(1,2)), \tag{22}$$

where the superscripts $^{(1)}$ and $^{(2)}$ denote, respectively, one- and two-electron operators, with the number between brackets beside each operator indicating the electrons on which the operator acts. Assuming a basis of independent electrons, we can write:

$$2\mathrm{Tr}_{e,2}(\hat{\chi}^{B(2)}(2)\hat{\rho}_e^{(2)}(1,2)) = -2\hat{\rho}_e^{(1)}(1)\hat{\chi}^{B(1)}(1)\hat{\rho}_e^{(1)}(1) + 4\hat{\rho}_e^{(1)}(1)\mathrm{Tr}(\hat{\chi}^{B(1)}(1)\hat{\rho}_e^{(1)}(1)). \tag{23}$$

In this way, we arrive to the equation of motion for our one-electron density operator:

$$\mathrm{i}\,\hbar\frac{d\hat{\rho}_e}{dt} = [\hat{H}_e, \hat{\rho}_e] + e[\hat{x}, [\hat{\chi}^A, \hat{\rho}_e]] + e[\hat{x}, (\{\hat{\chi}^B, \hat{\rho}_e\} + 4\hat{\rho}_e\mathrm{Tr}(\hat{\chi}^B\hat{\rho}_e) - 2\hat{\rho}_e\hat{\chi}^B\hat{\rho}_e)]. \tag{24}$$

Effect of band bending

Figure S1 presents the current (left panel) and the emitted power (right panel) in the steady state, for a semiconducting chain of gap 2 eV and an applied bias of 3 V. The behavior depends qualitatively on the self-consistency: in its absence, the response of the system is essentially metallic, as expected when the bias exceeds the band gap. It can be seen that the current, of around 50 μA, is not too different from the one obtained for the metallic wire at 1 V (blue curve in Figure 2 of main text), since at a

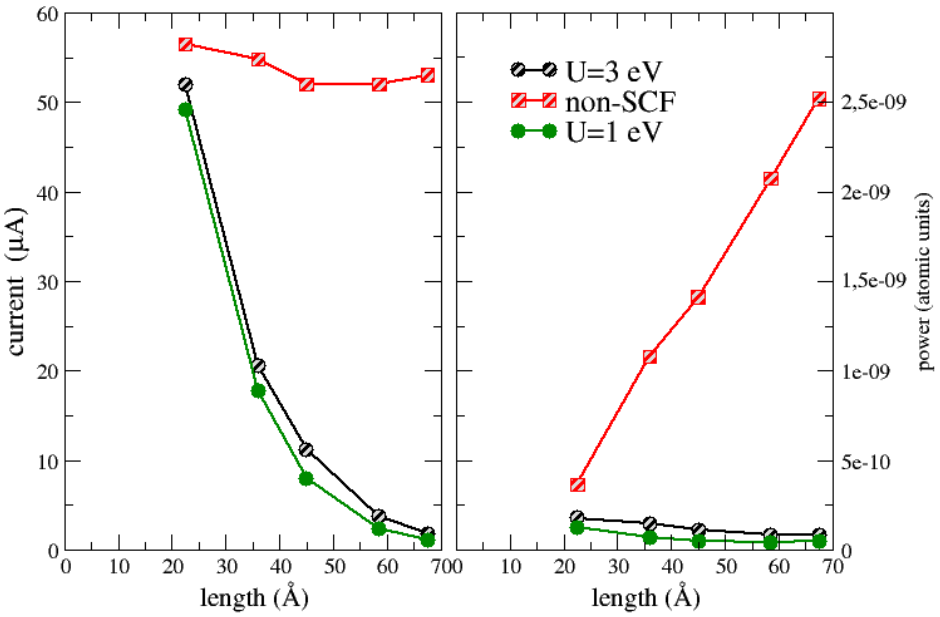

FIG. S1. Steady-state current (left) and power (right) for a semiconducting chain of band gap = 1 eV and applied bias 3 V. Results for different values of the U parameters are shown.

bias of 3 V, the accessible range for conduction in the semiconductor, not blocked by the 2 V gap, is precisely 1 V.

In the presence of self-consistency, conduction turns to a tunneling mechanism ascribable to the band-bending (Figure 7 of main text). It is manifest that the value of the U parameter has a minor impact on the current and the electroluminescence, at least above 1 eV, where the self-consistent effect has reached saturation.

Figure S2 illustrates the incidence of applied bias on band bending, through the magnitude of the onsite energies on the boundaries of the polymer. The plotted energy values include a factor of 2, to reflect the chemical potential difference. It is seen that the onsite energy is not a continuous function of the bias, but exhibits a stepped dependence, suggesting that, at least within that interval, the electronic structure can adopt a finite number of solutions.

Through the band-bending, the self-consistent or mean-field electron-electron interaction of this model is responsible for capturing some important physics. Aside from producing tunneling transport

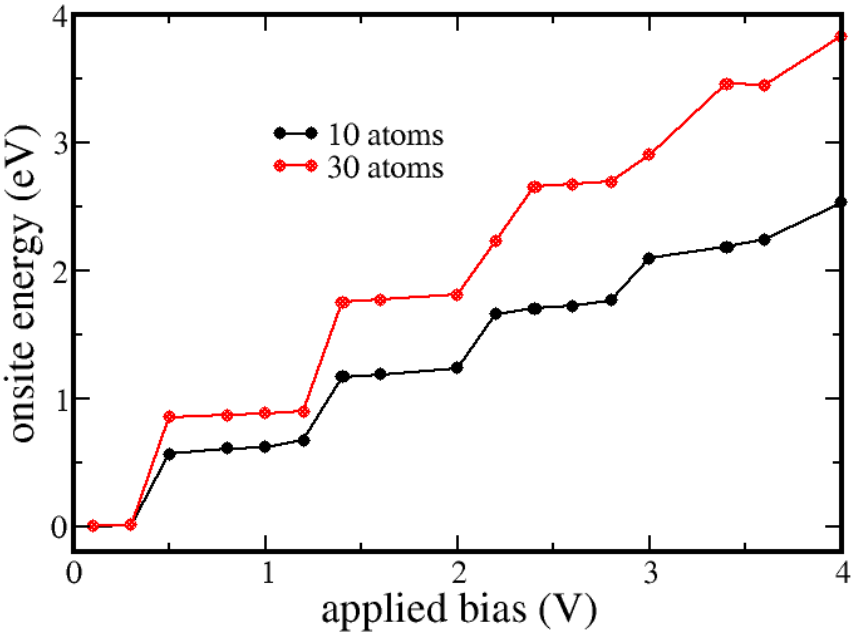

FIG. S2. Onsite energy (×2) of the terminal atom of the chain, as a function of the applied bias, for two different semiconducting polymers.

for a bias above the band gap, as discussed above, it can recreate under certain conditions negative differential resistance, as shown in section III.B of main text. Moreover, it gives rise to molecular rectification, an effect that is not observed in our simulations if the self-consistent contribution is removed. This is illustrated in Figure S3, which shows the IV curve for a polymer with asymmetric junctions having two different strengths assigned to the right and left electrode-molecule coupling terms, of -0.5 eV and -2.5 eV respectively. Without self-consistency, for U=0, the polarity does not affect the current. Instead, when the self-consistent electron interaction is switched on in the Hamiltonian with U=3 eV, the distinct intensification of the band-bending on the negative and positive electrodes introduces a dependence of the current on the sense of the electron flow. The left panel depicts the IV plots for a polymer of 10 atoms with and without self-consistency in the Hamiltonian. On the right panel, we show in black and red circles the difference between the negative and positive branches for U=0 (symmetric response) and U=3 eV, respectively. For the latter, a difference of nearly 10% between the backward and forward currents at 3 V attests the rectification arising from the self-consistent treatment.

The green curve represents the deviation of the positive branch for U=3 eV from the non-self-consistent case.

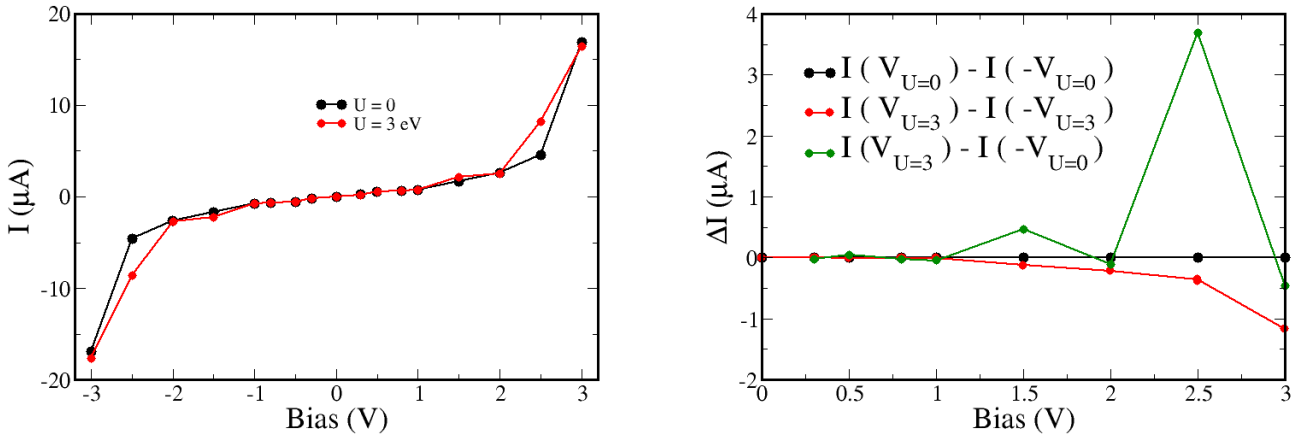

FIG. S3. Steady-state current as a function of bias, for the semiconducting polymer of 10 atoms with and without self-consistent interactions. The right panel shows the difference between the positive and negative branches in the presence (red) and in the absence (black) of self-consistency, and also the deviation of the positive branch obtained with U=3 eV from the branch with U=0.

Figure S4 shows for the semiconducting polymer the emitted power in the steady state as a function of length, reproducing the values obtained through the simulations that are depicted in Figure 10 of the main text, for applied biases of 1 and 3 V. In this case, we also plot the data resulting from the analytical model of equation 16. The parameters a and k were obtained from a fitting to the onsite energies as a function of length (Figure 8 of main text), whereas the value of the m factor was estimated from the power obtained for the metallic wires (Figure 4).

The better agreement at 3 V is expectable since the model becomes nearly independent from the a and k fitting. At 1 V, instead, the bending effect plays a major role, inducing a negative differencial resistance that falls outside the model's scope, which fails to predict the inversion of the curvature in that region. The positive curvature at low bias could be however reproduced by the model if the set of parameters were estimated using a different criterion. Importantly, there is not a single way to estimate the m parameter and for this reason the model can not be used in a quantitative sense in its present form. Yet, it is timely to acknowledge its usefulness to understand the trends revealed through the simulations.

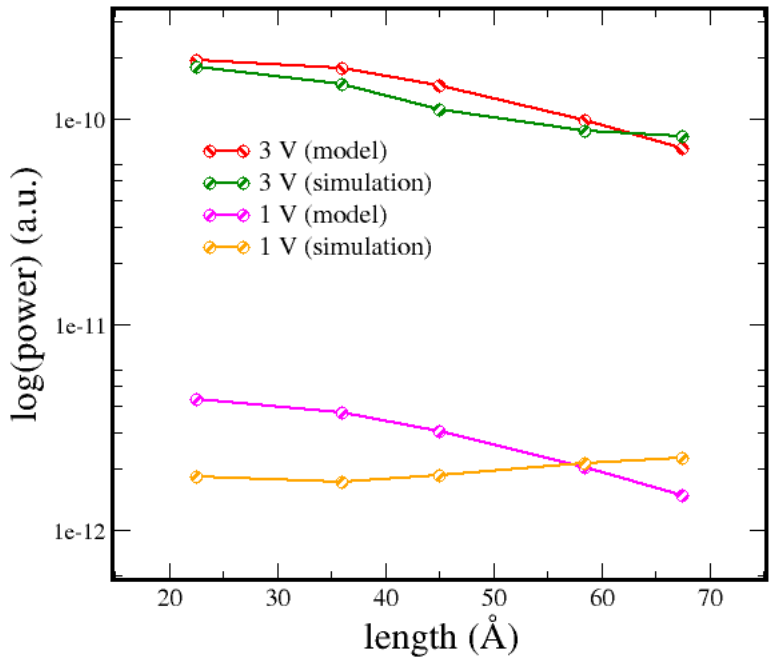

FIG. S4. Logarithm of the steady-state emitted power as a function of polymer length, for the semiconducting chain at two different applied biases. Also shown are the results from the model formulated in equation 16.